Electronic Supplementary Material (ESI) for Journal of Materials Chemistry C.

Supplementary information

Title: "Ultrathin flexible electronic device based on tunneling effect: a flexible ferroelectric tunnel junction"

Author(s): Pengfei Hou,[1,2,] KaiXin Yang,[1,2] Kaikai Ni,[1,2] Jiaxun Song,[1,2] Jinbin Wang,[1,2,†] Xiangli Zhong[1,2,‡] and Min Liao[1,2]

[1] School of Materials Science and Engineering, Xiangtan University, Hunan Xiangtan411105, China

[2] Key Laboratory of Low-dimensional Materials and Application Technology, Xiangtan University, Hunan Xiangtan 411105, China

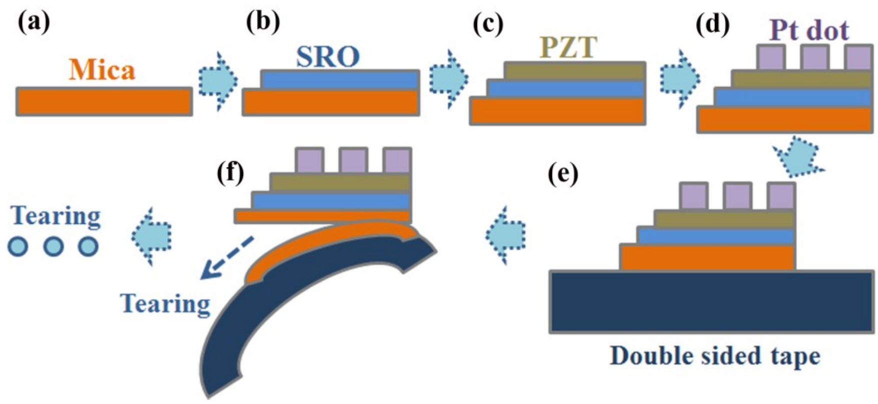

Figure S1. The preparation process of Flexible ferroelectric tunnel junction.

† *Corresponding author: Electronic mail* jbwang@xtu.ed.cn .
‡ *Corresponding author: Electronic mail* xlzhong@xtu.edu.cn .

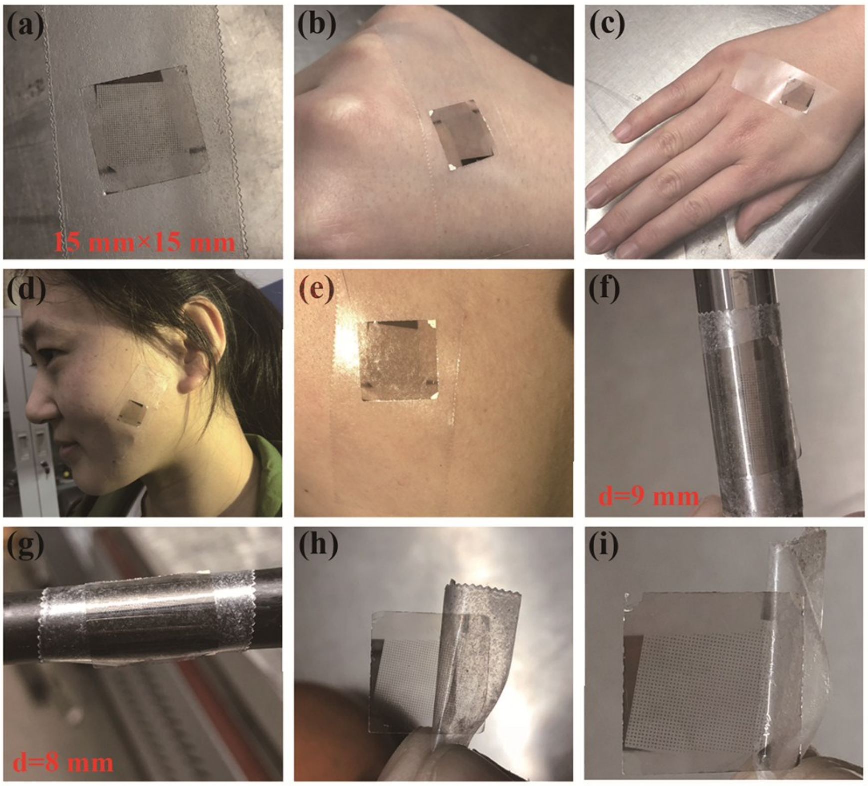

Figure S2. (a)-(g) Optical images showing the bending property of flexible ferroelectric tunnel junction arrays. **(a)** shows flexible ferroelectric tunnel junction arrays directly attached to a piece of double sticky tape. The area of the ferroelectric tunnel junction device is about 15 mm×15 mm. **(b)** shows flexible ferroelectric tunnel junction arrays directly attached to a tester's fist. **(c)** shows the relaxed fist with flexible ferroelectric tunnel junction arrays. **(d)-(e)** shows flexible ferroelectric tunnel junction arrays directly attached to a tester's face. **(f)-(g)** shows flexible ferroelectric tunnel junction arrays directly attached to pens with diameters of 9 mm and 8 mm. **(h)-(i)** shows the Mica substrate can be tore layer by layer by rolling up the double sticky tape with very large curvature.

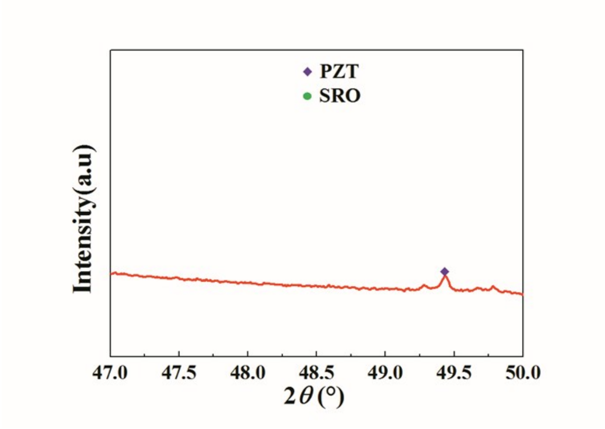

Figure S3. XRD patterns of PZT/SRO/Mica heterostructures at various 2θ.

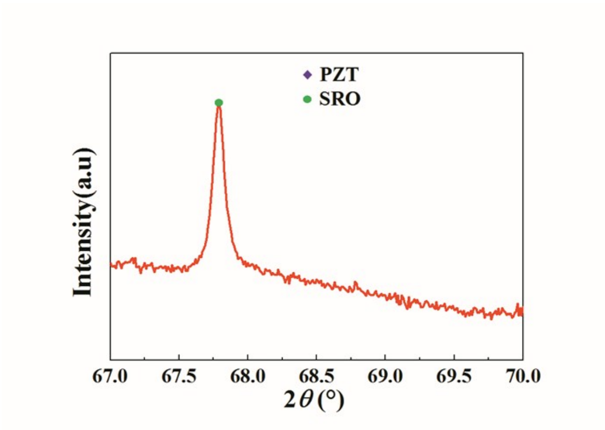

Figure S4. XRD patterns of PZT/SRO/Mica heterostructures at various 2θ.

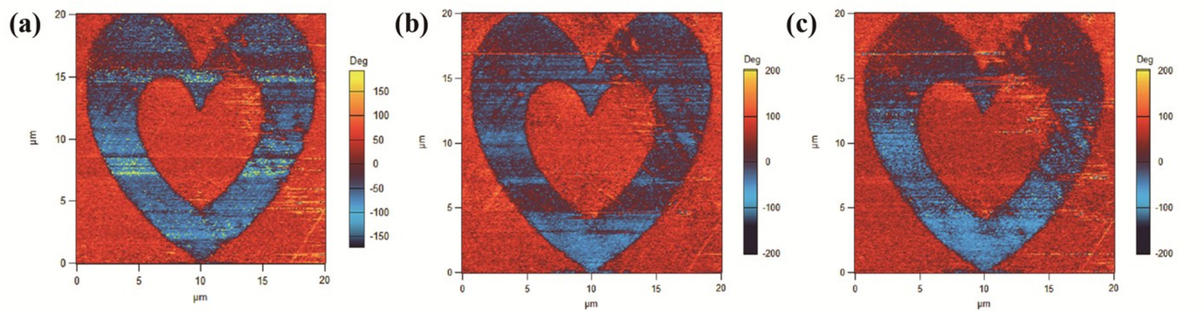

Figure S5. Distinct regions of opposite polarization in the PZT film can be seen in (a), (b) and (c).

(a) 0 h; (b) 1 h; (c) 2 h.

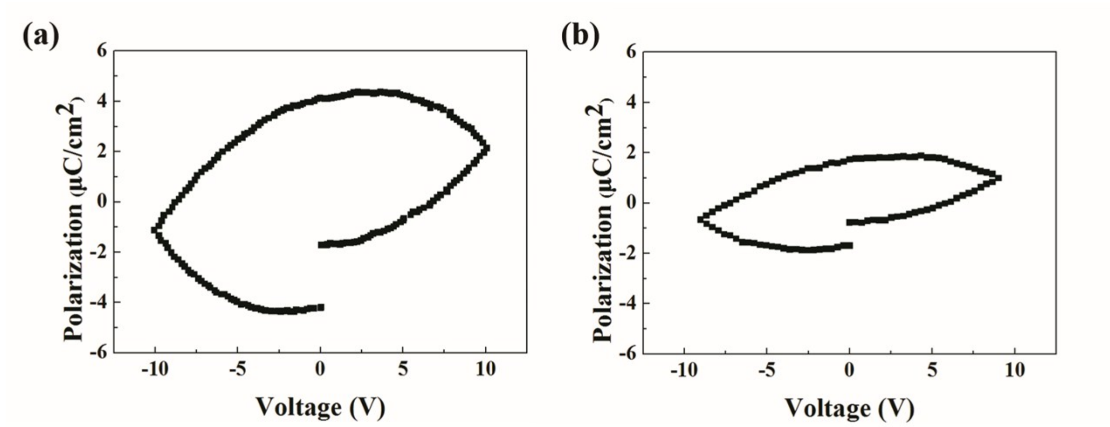

Figure S6. Hysteresis loops of flexible PZT thin film at various applied voltage.

(a) Relaxed state; (b) Bended state.

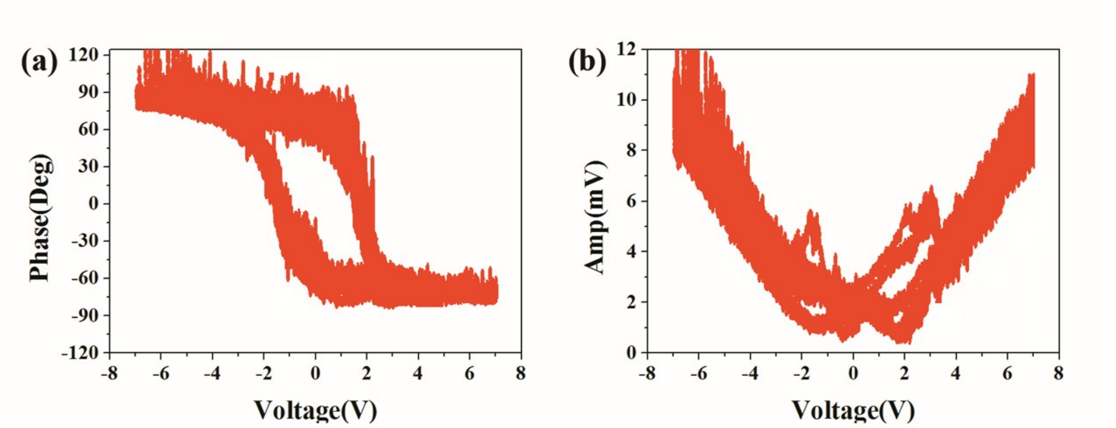

Figure S7. The hysteresis and amplitude loops.

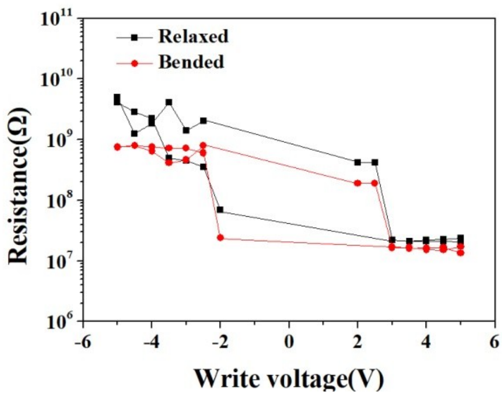

Figure S8. Resistance as a function of the writing pulse amplitude for the junction. The bottom electrode is grounded.

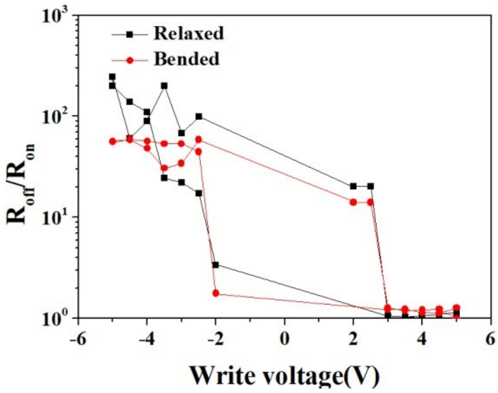

Figure S9. R_{OFF}/R_{ON} as a function of the writing pulse amplitude for the junction. The R_{ON} value is constant (it is the resistance value when the junction is written with voltage pulse of 5 V), and only the R_{OFF} value varies with the writing voltage.

Detailed calculated information

The current of the ferroelectric tunnel junction with 4 nm thick PZT film based on direct tunneling, Fowler-Nordheim tunneling and thermionic injection has been calculated as followings.

The PZT with a polarization P and a static permittivity ε_{stat} is sandwiched between SRO and Pt with different Thomas-Fermi screening lengths l_1 and l_2. A voltage V_0 is applied on the device and the resulting current I through the SRO/PZT/Pt heterostructure is calculated in dependence on the ferroelectric polarization direction. In fact, the resistance of SRO film is relative high, and the area of the sample is large. So the SRO film takes a large voltage, and a voltage V is applied on the PZT film really. The polarization P is perpendicular to the film surface, either pointing toward the contact where the voltage is applied ($P > 0$) after switching with a negative voltage or away from it ($P < 0$) after switching with a positive voltage.

The screening charge density Q_s, given by

$$Q_s = \frac{Pd}{\varepsilon_{stat}\left(\frac{l_1}{\varepsilon_{M,1}} + \frac{l_2}{\varepsilon_{M,2}}\right) + d} \tag{1}$$

The depolarization field E_{depol} and the change in the potential barriers $2\Delta\Phi_{\mathrm{i}}$ on polarization reversal inside the ferroelectric can be calculated from Thomas-Fermi screening.

$$E_{depol} = -\frac{(P - Q_s)}{\varepsilon_0 \varepsilon_{stat}}, \tag{2}$$

$$\Delta\Phi_i = \frac{l_i Q_s}{\varepsilon_0 \varepsilon_{m,i}} e, i = 1, 2, \tag{3}$$

The potential barrier without image force lowering is then given by

$$\Phi_{B,i} = \Phi_i \pm \Delta\Phi_i \tag{4}$$

where $\Phi_{1,2}$ is the barrier without polarization which might be different for different electrode. The upper sign (+) applies for Φ_1 (the barrier at the interfaces between SRO and the ferroelectric) and the lower sign (-) for Φ_2 (the barrier at the interfaces between metal Pt and the ferroelectric). The potential barrier Φ_{B} is the energy barrier which the electrons must overcome during transport across the SRO/PZT/Pt heterostructure, i.e., $\Phi_{\mathrm{B},1}$ for $V > 0$ and $\Phi_{\mathrm{B},2}$ for $V < 0$.

Applied field $E_{ap} = -V/d$, the field due to band alignment E_{band}, $E_{band} = \frac{\Phi_2 - \Phi_1}{ed}$.

However, here, we focus on the polarization dependence and introduce it by employing a model proposed by Zhuravlev et al.[1] We used the direct tunnel current density j_{DT} given by Gruverman et al.[2]

$$j_{DT} = C \frac{\exp\left[\alpha\left\{\left(\Phi_{B,2} - \frac{eV}{2}\right)^{3/2} - \left(\Phi_{B,1} + \frac{eV}{2}\right)^{3/2}\right\}\right]}{\alpha^2\left[\sqrt{\Phi_{B,2} - \frac{eV}{2}} - \sqrt{\Phi_{B,1} + \frac{eV}{2}}\right]^2} \sinh\left[\frac{3eV}{4}\alpha\left\{\sqrt{\Phi_{B,2} - \frac{eV}{2}} - \sqrt{\Phi_{B,1} + \frac{eV}{2}}\right\}\right] \tag{5}$$

Where $C = \dfrac{4em_{e,ox}}{9\pi^2\hbar^3}$, $\alpha = \dfrac{4d\sqrt{2m_{e,ox}}}{3\hbar(\Phi_{B,1} + eV - \Phi_{B,2})}$, $m_{e,ox}$ being the effective tunneling electron mass.

Thermionic injection describes the current which is due to charge carriers which overcome the potential barrier by thermal energy. The barrier height is lowered by image force lowering, called the Schottky effect.[3] The thermionic injection current density $j_{Schottky}$ can be described for sufficiently high voltages.

$$j_{Schottky} = A^{**}T^2 \exp\left[-\frac{1}{k_B T}\left(\Phi_B - \sqrt{\frac{e^3 E}{4\pi\varepsilon_0\varepsilon_{ifl}}}\right)\right] \tag{6}$$

Where A^{**} the effective Richardson's constant, and ε_{ifl} the permittivity of the ferroelectric responsible for image force lowering.

Fowler-Nordheim tunneling (FNT) is tunneling across a triangular-shaped potential barrier, which is formed by applying an electrical field E to a rectangular or trapezoidal barrier.[4] FNT is basically the same physical phenomena as direct tunneling, but in a different voltage regime.

$$j_{FN} = \frac{e^3 m_e}{8\pi h m_{e,ox}\Phi_B} E^2 \exp\left[-\frac{8\pi\sqrt{2m_{e,ox}}}{3he}\frac{\Phi_B^{3/2}}{E}\right] \tag{7}$$

In both the latter mechanisms the electric field E is the field responsible for band tilting. The parameters corresponding to PZT (d = 4 nm, ε_{stat} = 200, ε_{ifl} = 10, $m_{e,ox} = m_e$, and $A^{**} = 10^6$ A m^{-2} K^{-2}) and its interface with SRO (l_1 = 0.8Å, $\varepsilon_{M,1}$ = 8) and Pt [l_2 = 0.55 Å, and $\varepsilon_{M,2}$ = 2] were used. The P value of PZT is 4 μC/cm^2 at relaxed state, and 2 μC/cm^2 at bended state. When the device is at ON state, Φ_1 is 0.7 eV, and Φ_2 is 0.66 eV. When the device is at OFF state, Φ_1 is 1.2 eV, and Φ_2 is 0.8 eV. The final current is a combination of the three mechanisms. However, direct tunneling current is prominent at low voltage and Fowler–Nordheim tunneling dominates at large voltage. The calculated result is shown in figure S7, in which the current density has been changed to current and the diameter of the electrode is about 100 μm. In **figure S10**, the voltage is V_0, and V_0 is 12.5V, these prove that the SRO film takes a large voltage. The calculated results are fit the experimental result in **figure 7**.

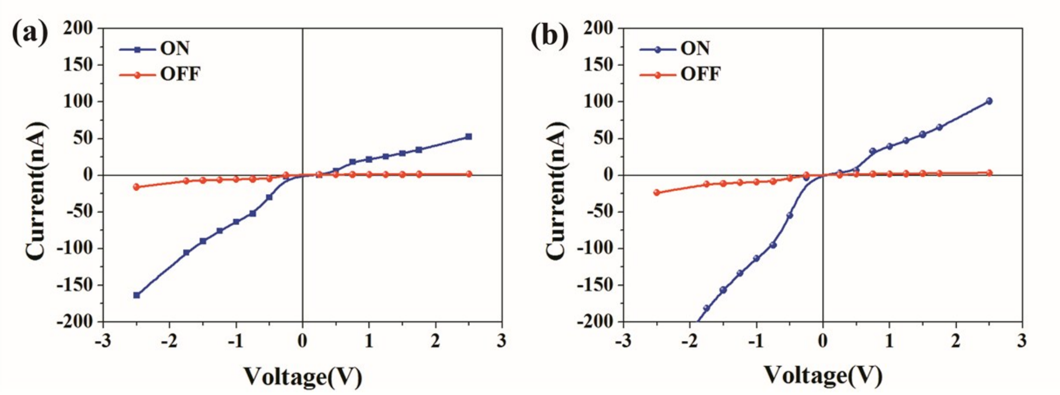

Figure S10. Calculated *I-V* curves of the ferroelectric tunnel junction with 4 nm thick PZT film. (a) Relaxed state; (b) Bended state.

Table 1 Comparison of the flexible/non-flexible junctions.

Ref.	Type	Ferroelectric material	Organic	Flexible	Switching ratio
34	Tunnel junction	$BaTiO_3$	No	No	~6.0×10^{6}
44	Transistor	PVDF-TrFE	Yes	Yes	10^{4}~10^{8}
45	Transistor	PVDF-TrFE	Yes	Yes	~10^{5}
46	Transistor	PVDF-TrFE	Yes	No	~10^{5}
48	Tunnel junction	$BaTiO_3$	No	No	10^{4}~10^{7}
This paper	Tunnel junction	PZT	No	Yes	100

Table 2 The R_{OFF}/R_{ON} as a function of the radius of curvature

Curvature radius	Highest on/off ratio	Average on/off ratio
(Relaxed)	2.45×10^{4}%	1.08×10^{4}%
4.5mm	5.6×10^{3}%	1.5×10^{3}%
4 mm	6.7×10^{2}%	2.4×10^{2}%

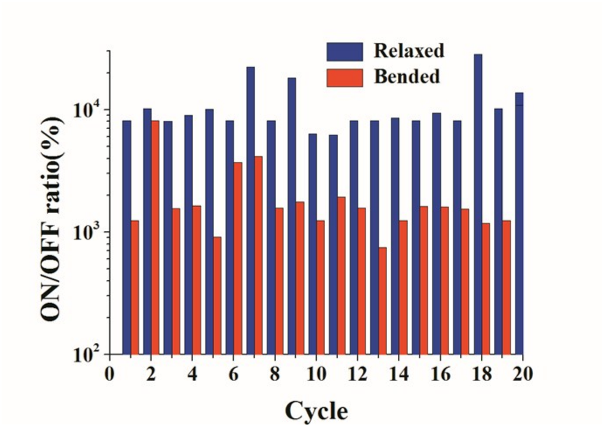

Figure S11. Switch ratio of as a function of switch cycles.

References

[1] M. Y. Zhuravlev, R. F. Sabirianov, S. S. Jaswal, and E. Y. Tsymbal, Giant electroresistance in ferroelectric tunnel junctions, *Phys. Rev. Lett.* 94, 246802 (2005).

[2] A. Gruverman, et al. Tunneling electroresistance effect in ferroelectric tunnel junctions at the nanoscale, Tsymbal, *Nano Lett.* 9, 3539 (2009).

[3] S. M. Sze, K. K. Ng, Physics of semiconductor devices, *John wiley & sons* (2006).

[4] R. H. Fowler, and L. Nordheim, Electron emission in intense electric fields, *Proc. R. Soc. London, Ser. A* 119, 173 (1928).